The Astrophysical Journal, 591:515–525, 2003 July 10
© 2003. The American Astronomical Society. All rights reserved. Printed in U.S.A.

CLUSTER SUNYAEV-ZELDOVICH EFFECT SCALING RELATIONS

Ian G. McCarthy,[1] Arif Babul,[1,2] Gilbert P. Holder,[3] and Michael L. Balogh[4]
Received 2002 October 2; accepted 2003 February 5

ABSTRACT

X-ray observations of an "entropy floor" in nearby groups and clusters of galaxies offer evidence that important nongravitational processes, such as radiative cooling and/or "preheating," have strongly influenced the evolution of the intracluster medium (ICM). We examine how the presence of an entropy floor modifies the thermal Sunyaev-Zeldovich (SZ) effect. A detailed analysis of scaling relations between X-ray and SZ effect observables and also between the two primary SZ effect observables is presented. We find that relationships between the central Compton parameter and the temperature or mass of a cluster are extremely sensitive to the presence of an entropy floor. The same is true for correlations between the integrated Compton parameter and the X-ray luminosity or the central Compton parameter. In fact, if the entropy floor is as high as inferred in recent analyses of X-ray data, a comparison of these correlations with both *current* and future SZ effect observations should show a clear signature of this excess entropy. Moreover, because the SZ effect is redshift independent, the relations can potentially be used to track the evolution of the cluster gas and possibly discriminate between the possible sources of the excess entropy. To facilitate comparisons with observations, we provide analytic fits to these scaling relations.

Subject headings: cosmic microwave background — cosmology: theory — galaxies: clusters: general — X-rays: galaxies: clusters

1. INTRODUCTION

Correlations between the global X-ray properties of galaxy clusters have proven to be important probes of the intracluster medium (ICM). Studies of the relation between the X-ray luminosity (L_X) and the emission-weighted temperature (T_X) have been particularly powerful. Numerical simulations and analytic models that take into account the effects of gravity and shock heating of the gas only (i.e., the so-called self-similar models) predict that $L_X \propto T_X^2$ for massive clusters, yet the observed relation is much steeper: $L_X \propto T_X^{2.6-3.0}$ (e.g., Markevitch 1998; Allen & Fabian 1998; Arnaud & Evrard 1999). A number of other observed X-ray scaling relations, for example, the total cluster mass (M_{tot})-T_X and total ICM mass (M_{gas})-T_X relations, have also recently been shown to deviate from their predicted scalings (e.g., Horner, Mushotzky, & Scharf 1999; Ettori & Fabian 1999; Mohr, Mathiesen, & Evrard 1999; Vikhlinin, Forman, & Jones 1999; Nevalainen, Markevitch, & Forman 2000; Finoguenov, Reiprich, & Böhringer 2001; McCarthy, Babul, & Balogh 2002, hereafter MBB02). These discrepancies between theory and observations have motivated a number of authors to examine the potential role of "additional" gas physics. For example, the heating of the ICM by galactic winds and/or quasar outflows has been investigated by Kaiser (1991) and also by a whole host of subsequent authors (e.g., Evrard & Henry 1991; Bower 1997; Balogh, Babul, & Patton 1999; Wu, Fabian, & Nulsen 2000; Loewenstein 2000; Tozzi & Norman 2001; Borgani et al. 2001; Babul et al. 2002, hereafter BBLP02; MBB02; Nath & Roychowdhury 2002; Lloyd-Davies, Bower, & Ponman 2002). Recently, the effects of radiative cooling on X-ray scaling relations have also been explored (e.g., Bryan 2000; Voit & Bryan 2001; Wu & Xue 2002; Thomas et al. 2002; Voit et al. 2002; Davé, Katz, & Weinberg 2002). These studies find that both heating and cooling can act in a similar manner, by raising the mean entropy of the intracluster gas and, in some cases, establishing a core in the entropy profile. This, in turn, modifies the X-ray scaling relations of clusters and ameliorates, or possibly eliminates, the discrepancies between theory and observations. It also potentially explains the emerging observational evidence for an "entropy floor" in nearby groups and low-mass clusters (Ponman, Cannon, & Navarro 1999; Lloyd-Davies, Ponman, & Cannon 2000).

Thus far, X-ray observations alone have provided evidence for the entropy floor, and it has come almost entirely from low-redshift ($z \lesssim 0.2$) groups/clusters. Observations of higher redshift clusters are hindered by cosmological dimming [the bolometric X-ray surface brightness of a cluster scales as $(1+z)^{-4}$]. An additional, *independent* probe that could be used to confirm the presence of this excess entropy in low/intermediate-redshift clusters and also to provide new tests for their high-redshift counterparts would be quite useful. Here we show that scaling relations based on the thermal Sunyaev-Zeldovich (SZ) effect (Sunyaev & Zeldovich 1970, 1980) can provide such a probe.

The SZ effect is a fractional change in the temperature/intensity of the cosmic microwave background (CMB) caused by the inverse Compton scattering of CMB photons off high-energy electrons in the ICM. On average, the photons gain a small amount of this energy from the scatterings, and this results in a slight spectral distortion of the CMB toward clusters. At frequencies of $\nu \lesssim 218$ GHz, the SZ effect appears as a decrement in the temperature of the CMB, while at higher frequencies it appears as an increment. The magnitude of the SZ effect is determined by the integrated gas pressure along the line of sight through the cluster. Since

[1] Department of Physics and Astronomy, University of Victoria, P.O. Box 3055, Victoria, BC V8P 1A1, Canada; mccarthy@beluga.phys.uvic.ca.
[2] CITA Senior Fellow.
[3] School of Natural Sciences, Institute for Advanced Study, Princeton, NJ 08540.
[4] Department of Physics, University of Durham, Science Laboratories, South Road, Durham DH1 3LE, UK.

heating/cooling modifies the entropy of the gas, it should be expected that the gas pressure and, thus, the SZ effect will also be modified by these processes. Therefore, it can be expected that SZ effect scaling relations will tell us something about the entropy history of the gas. Unlike the X-ray surface brightness of a cluster, the SZ effect is not subject to cosmological dimming and can be used to study the effects of excess entropy in the ICM out to arbitrarily high redshift. This makes scaling relations based on the SZ effect particularly interesting and attractive tests.

Traditionally, detecting and mapping the SZ effect have been quite difficult. This is because the effect is very weak, with typical beam-averaged decrements in the CMB temperature of only a few hundred μK (see Birkinshaw 1999 for a recent compilation). Recently, however, extraordinary leaps in detector technology and new observing strategies have allowed observers to make reliable and routine pointed observations of the effect (for recent data see, e.g., Grego et al. 2001; Grainge et al. 2002; Reese et al. 2002). With this advance, we feel that a detailed study of SZ effect scaling relations and what new insights they can give us on the thermal and spatial characteristics of the ICM, especially in high-redshift clusters, is timely.

In this paper we construct SZ effect scaling relations for massive clusters both with and without excess entropy and focus on how these correlations are modified by the presence of an entropy floor. Along the way, we also discuss the potential for both current and future observations to measure these relations and constrain the entropy floor level. Constraining the entropy floor level out to high redshift could possibly yield information about the source(s) of the excess entropy, whether it be "preheating" by quasar outflows, radiative cooling, or some other nongravitational process. In a companion paper (McCarthy et al. 2003) we compare the scaling relations derived here to high-redshift SZ effect data from the literature.

To date, only a few other theoretical studies have investigated the role of excess entropy on the SZ effect. White, Hernquist, & Springel (2002), Springel, White, & Hernquist (2001), da Silva et al. (2001), Cavaliere & Menci (2001), and Holder & Carlstrom (2001) have all looked at how *universal* SZ effect properties, such as the SZ effect angular power spectrum, SZ effect cluster source counts, and/or the mean universal Compton parameter, are modified by an entropy floor. However, measurements of most of these quantities are not feasible with current instrumentation; therefore, estimates of the entropy floor level of clusters via observations of universal SZ effect quantities will have to wait until the next generation of instruments (e.g., the Sunyaev-Zeldovich Array [SZA], the Arcminute Microkelvin Imager [AMI], and the Array for Microwave Background Anisotropy [AMiBA]) come on-line. In a spirit similar to that of the present study, however, Holder & Carlstrom (2001) and Cavaliere & Menci (2001) have also examined a few SZ effect scaling relations for *individual* clusters. We briefly compare our findings to the results of these two studies in § 5.

The present paper is outlined as follows. In § 2 we briefly describe the analytic cluster models developed in BBLP02 and employed here. In § 3 we discuss in a general sense how and why entropy injection is expected to influence the SZ effect and how this can be explored with current and future observations through comparisons with predicted scaling relations. In § 4 we derive theoretical scaling relations based on SZ effect observables and quantify how excess entropy modifies these relations. We start by examining scaling relations consisting only of SZ effect observables. These relations are most interesting because they potentially offer a completely (X-ray–)independent way of probing the intracluster gas. Next, we explore scaling relations between the various SZ effect observables and a cluster's mass. These relations, too, can potentially be measured independent of X-ray observations, since clusters can be weighed via gravitational lensing or galaxy velocity dispersion measurements. Finally, we construct and analyze scaling relations between the various SZ effect and X-ray observables (i.e., X-ray luminosity and emission-weighted temperature). In § 5 we discuss and summarize our findings.

The models we consider below were developed in a flat ΛCDM cosmology with $h = 0.75$, $\Omega_m = 0.3$, and $\Omega_b = 0.020\ h^{-2}$ (Burles, Nollett, & Turner 2001). They are computed for a number of different entropy floor levels spanning the range $K_0 \approx 100$–430 keV cm^2. This is approximately the range found to match the observed L_X-T_X relations of both groups and hot clusters (e.g., Ponman et al. 1999; Lloyd-Davies et al. 2000; Tozzi & Norman 2001; BBLP02; MBB02). We work in physical units throughout the paper (e.g., $M_\odot$ rather than $h^{-1}\ M_\odot$).

2. GALAXY CLUSTER MODELS

Since an in-depth discussion of the cluster models can be found in BBLP02, we present only a brief description of the models here. We note that the model clusters derived here represent high-mass ($M_{\rm tot} \gtrsim 3 \times 10^{14}\ M_\odot$), high-temperature ($T_X \gtrsim 3$ keV) clusters only. Such a range reflects all of the clusters observed to date through the SZ effect and is approximately the range expected to be probed by upcoming interferometric surveys (e.g., Holder et al. 2000).

2.1. *The Self-similar Model*

To mimic the standard self-similar result deduced from numerical simulations, we implement the "isothermal" model of BBLP02. In this model, the ICM is assumed to be isothermal and is in hydrostatic equilibrium with the dark halo potential. The distribution of the dark matter in these clusters is assumed to be the same as found in recent high-resolution numerical simulations (Moore et al. 1998; Lewis et al. 2000). This model will serve as our "baseline" model for assessing how an entropy floor modifies the SZ effect. The isothermal model has been tested extensively (BBLP02; MBB02) to make sure it provides a good match to the results of genuine self-similar numerical simulations, such as those done by Evrard, Metzler, & Navarro (1996).

2.2. *The Entropy Floor Models*

To test the effects of an entropy floor on the SZ effect, we make use of the entropy injection (preheated) models of BBLP02. The models can be summarized as follows: the dominant dark matter component, which is unaffected by the energy injection, collapses and virializes to form bound halos. The distribution of the dark matter in such halos is assumed to be the same as for the self-similar clusters described above. While the dark component is unaffected by energy injection, the collapse of the baryonic component is hindered by the pressure forces induced by entropy injection. If the maximum infall velocity due purely to gravity of

the dark halo is subsonic, the flow will be strongly affected by the pressure and will not undergo accretion shocks. It is assumed that the baryons will accumulate onto the halos *isentropically* at the adiabatic Bondi accretion rate (as described in Balogh et al. 1999). This treatment, however, is only appropriate for low-mass halos. If the gravity of the dark halos is strong enough (as it is expected to be in the hot clusters being considered here) that the maximum infall velocity is transonic or supersonic, the gas will experience an additional (generally dominant) entropy increase as a result of accretion shocks. In order to trace the shock history of the gas, a detailed knowledge of the merger history of the cluster/group is required but is not considered by BBLP02. Instead, it is assumed that at some earlier time the most massive cluster progenitor will have had a mass low enough such that shocks were negligible in its formation, similar to the low-mass halos discussed above. This progenitor forms an isentropic gas core of radius r_c at the cluster center. The entropy of gas outside of the core, however, will be affected by shocks. Recent high-resolution numerical simulations suggest that the "entropy" profile for gas outside this core can be adequately represented by a simple analytic expression given by $\ln K(r) = \ln K_0 + \alpha \ln(r/r_c)$ (Lewis et al. 2000), where $K \equiv kT_e n_e^{-2/3}$. For the massive, hot clusters ($T_X \gtrsim 3$ keV) of interest here, $\alpha \sim 1.1$ (Tozzi & Norman 2001; BBLP02).

Following this prescription and specifying the parameters r_c, $\rho_{gas}(r_c)$, and α (as discussed in BBLP02) completely determine the models. Under all conditions, the gas is assumed to be in hydrostatic equilibrium within the dark halo potential. The complicated effects of radiative cooling are neglected by these models.

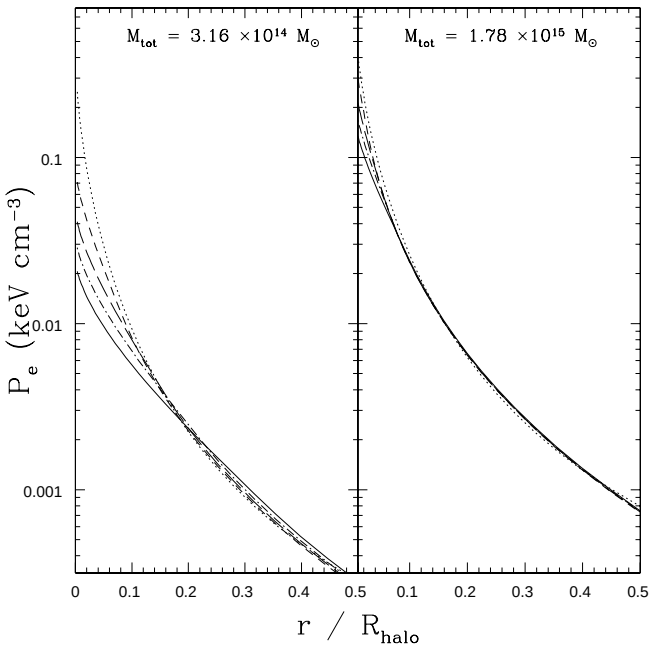


FIG. 1.—Effects of an entropy floor on cluster pressure profiles. *Left:* Cluster with total mass $M_{tot} = 3.16 \times 10^{14}\ M_\odot$. *Right:* Cluster with total mass $M_{tot} = 1.78 \times 10^{15}\ M_\odot$. The dotted line is the standard self-similar result. The short-dashed, long-dashed, dot-dashed, and solid lines represent the models of BBLP02 with entropy floor constants of $K_0 = 100$, 200, 300, and 430 keV cm^2, respectively.

3. ENTROPY INJECTION AND THE SZ EFFECT

The amplitude of the SZ effect is directly proportional to the "Compton parameter" (y), which is given by

$$y(\theta) = \frac{\sigma_T}{m_e c^2} \int P_e(\boldsymbol{r}) dl \ , \qquad (1)$$

where θ is the projected position from the cluster center, σ_T is the Thomson cross section, and $P_e(\boldsymbol{r}) \equiv n_e(\boldsymbol{r}) kT_e(\boldsymbol{r})$ is the electron pressure of the ICM at the three-dimensional position $\boldsymbol{r}$. The integral is performed over the line of sight (l) through the cluster.

All of the physics of the SZ effect is contained within the Compton parameter. It is the SZ effect analog of the X-ray surface brightness of a cluster and is a measure of the average fractional energy gain of a photon due to inverse Compton scattering while passing through a cloud of gas (in this case, the ICM) with an electron pressure profile of $P_e(\boldsymbol{r})$. As discussed by BBLP02 and MBB02, the presence of excess entropy will modify both a cluster's density and temperature profiles. In the case in which it is preheating that gives rise to an entropy core, as in the present study, the temperature of the gas near the center of the cluster is increased and, therefore, so is the global emission-weighted temperature of the cluster (e.g., Fig. 1 of MBB02). At the same time, the density of the gas at the cluster center is dramatically reduced (e.g., Fig. 2 of MBB02). It turns out that, relatively speaking, preheating has a stronger influence on the density than it does on the temperature, at least at the centers of massive clusters. The result is that the gas pressure in central regions of a cluster is reduced by preheating and, consequently, so is the cluster's Compton parameter. To demonstrate this, we plot cluster pressure profiles ($z = 0.2$) for several values of the entropy floor in Figure 1 (R_{halo} is the radius of the cluster). The addition of an entropy floor leads to a decrease in the gas pressure near the cluster core. The gas pressure in the outer regions of the clusters, however, remains relatively unchanged as the entropy increase due to gravitational shock heating dominates the nongravitational entropy injection. Also of note is that the *relative* difference between the various models is greatest for the lower mass cluster. This is expected since the lower mass cluster has a shallower potential well and, thus, is more strongly influenced by the presence of an entropy floor.

With an entropy floor significantly affecting the pressure of the ICM near the center of a cluster, the Compton parameter will be most strongly modified if it is evaluated within the smallest possible projected radius [i.e., the *central* Compton parameter, $y(\theta = 0) \equiv y_0$]. Integrating (or averaging) the Compton parameter within larger projected radii (for example, R_{halo}, the radius of the cluster), on the other hand, will diminish (although not completely remove) the effects of entropy injection. Which of these quantities, the central or integrated Compton parameters, will be the most useful for constructing scaling relations that are sensitive to the value of K_0 will depend on which other cluster observables are used in the relations. For example, in § 4 we show that a comparison of y_0 with T_X provides a more sensitive test of entropy injection than a comparison of the integrated Compton parameter with T_X. On the other hand, a scaling relation between the integrated Compton parameter and L_X is more sensitive to the entropy floor level than is

a scaling relation between y_0 and L_X. Ultimately, one would like to directly image the entire cluster out to the virial radius with high angular resolution and directly compare theoretical models to the images over the entire cluster profile.

The observability of these quantities will obviously depend on the details of the instrument and observing strategy. Generically, observations of the SZ effect filter large-scale emission, while finite resolution smears out small-scale structures. Fitting to a model (such as the isothermal β model; Cavaliere & Fusco-Femiano 1976, 1978) provides a method for effectively deconvolving these effects and estimating the central and integrated Compton parameters, but it is important to keep in mind that such quantities are inferred and model dependent. Provided that the smallest angular scale resolved is comparable to the typical scale over which the cluster varies, the inferred y_0 will be reliable, while inferred integrated Compton parameters will not be reliable when extrapolated beyond the filtering scale of the observations. For current interferometric observations (such as those obtained with the Berkeley-Illinois-Maryland Association [BIMA] and Owens Valley Radio Observatory [OVRO] arrays and the Ryle telescope), the highest angular resolution for SZ measurements is typically smaller than the core radius of most clusters observed to date ($\sim 30''$), while the typical large-scale filtering becomes important on scales larger than about $2'$. Therefore, it can be expected that the inferred values of y_0 should be reasonably accurate while any integrated Compton parameter/flux density reported on scales larger than $2'$ will be suspect.

In recognition of the above, we construct scaling relations between the central Compton parameter, the integrated Compton parameter within the central $1'$ (which is a conservative choice for the filtering scale of current interferometers), and various X-ray observables. However, we also explore relations involving the integrated Compton parameter within $R_{\rm halo}$, as future experiments, such as SZA, will probe angular scales larger than that of current experiments.

4. SZ EFFECT SCALING RELATIONS

4.1. *100% SZ Effect: The S_ν-y_0 Relation*

We start our discussion of SZ effect scaling relations by first examining relations between SZ effect quantities only (i.e., the central and integrated Compton parameters). In principle, these relations are completely independent of X-ray results, in that the latter depend on the combination of $n_e^2\epsilon(T_e)$ [where $\epsilon(T_e)$ is the X-ray emissivity] whereas the SZ effect depends on n_eT_e. For this reason, scaling relations that depend only on SZ effect quantities have the potential of providing new insights into both the thermal and spatial properties of the ICM. As such, we will invest a little bit more effort discussing and expanding on the nature of these relations than the SZ effect–X-ray relations discussed later in §§ 4.2 and 4.3.

First, because the SZ effect flux density of a cluster is most commonly reported in observational studies and not the integrated Compton parameter, we convert the integrated Compton parameter (symbolized as $y_{\rm int}$), which is given by

$$y_{\rm int}(\leq\theta) = 2\pi\int_0^\theta y(\theta')\theta'\,d\theta' \ , \tag{2}$$

into flux density (S_ν) via

$$S_\nu = j_\nu(x)y_{\rm int} \ , \tag{3}$$

where $j_\nu(x)$ describes the shape of the SZ effect spectrum and is a function of the dimensionless frequency $x = h\nu/kT_{\rm CMB}$. The mean temperature of the present-day CMB, $T_{\rm CMB}$, is 2.728 K (Fixsen et al. 1996) and $j_\nu(x) = 2(kT_{\rm CMB})^3 \times (hc)^{-2}f_\nu(x)$, with

$$f_\nu(x) = \frac{x^4e^x}{(e^x-1)^2}\left[\frac{x}{\tanh(x/2)} - 4\right] \ , \tag{4}$$

where $f_\nu \approx -2x^2$ at long wavelengths (the Rayleigh-Jeans limit).

Since our aim here is to achieve a *physical* understanding of the relationship between S_ν and y_0, we remove the frequency dependence of the integrated SZ effect flux density by dividing it by the quantity f_ν given in equation (4). Then a comparison of the quantity S_ν/f_ν with genuine observations at any observing frequency ν can be made simply by multiplying by the conversion factor f_ν. For reasons discussed in § 3, we investigate the frequency-independent SZ effect flux density within a fixed angular radius of $1'$ (which we symbolize as $S_{\nu,{\rm arc}}/f_\nu$) and within $R_{\rm halo}$, the radius of the cluster (which we symbolize as $S_{\nu,{\rm halo}}/f_\nu$).

In Figure 2 we plot scaling relations between the (frequency-independent) SZ effect flux densities and the central Compton parameter. The dotted lines are the self-similar results. The short-dashed, long-dashed, dot-dashed, and solid lines represent the results of the models of BBLP02 with entropy floor constants of $K_0 = 100$, 200, 300, and 430 keV cm^2, respectively. The top panel is for the SZ effect flux density within the central $1'$, while the bottom panel is the

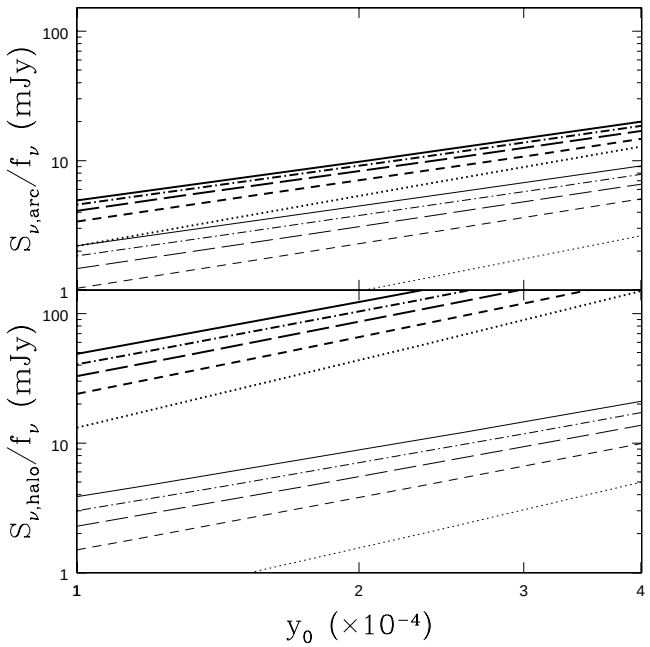


FIG. 2.—Comparison of the S_ν/f_ν-y_0 relations. The short-dashed, long-dashed, dot-dashed, and solid lines represent the models of BBLP02 with entropy floor levels $K_0 = 100$, 200, 300, and 430 keV cm^2, respectively. The dotted lines are the isothermal self-similar result. The thick lines are for $z = 0.2$, and the thin lines are for $z = 1.0$. *Top:* SZ effect flux density within the central $1'$. *Bottom:* Total SZ effect flux density of the cluster.

total SZ effect flux density of the cluster (out to $R_{\rm halo}$). The thick lines are for $z = 0.2$, and the thin lines are for $z = 1.0$.

We start by considering the dependence of $S_{\nu,\rm arc}/f_\nu$-y_0 on K_0 and z in the top panel of Figure 2. First, as discussed in § 3, entropy injection leads to a decrease in the gas pressure near the cluster core (Fig. 1). This, in turn, reduces the magnitude of both $S_{\nu,\rm arc}/f_\nu$ and y_0. However, the relative reduction in both of these quantities is not equal. $S_{\nu,\rm arc}/f_\nu$ is derived within larger physical radii than y_0 and, therefore, is less affected by the entropy floor. The result is an increase in the normalization of the $S_{\nu,\rm arc}/f_\nu$-y_0 relation as the value of K_0 is increased. For example, at $z = 0.2$, a cluster with a fixed value $\log y_0 \approx -3.7$ ($\Delta T_0 \approx -1060$ μK at 30 GHz) will have an integrated decrement of $S_{\nu,\rm arc}/f_\nu \approx 5.5$ mJy ($S_\nu \approx -11$ mJy at 30 GHz) if no entropy floor is present but will have $S_{\nu,\rm arc}/f_\nu \approx 10$ mJy ($S_\nu \approx -20$ mJy at 30 GHz) if $K_0 \approx 430$ keV cm^2. Furthermore, this trend is amplified at higher redshifts since the SZ effect flux density within a fixed angular size probes larger physical regions at higher redshifts (and, therefore, is less affected by the entropy floor). Compare the difference between the models for the $z = 0.2$ lines and the $z = 1.0$ lines, for example.

The slope of the $S_{\nu,\rm arc}/f_\nu$-y_0 relation is also modified by the presence of an entropy floor. For example,[5] at $z = 0.2$ and 1.0, respectively, the self-similar model approximately predicts

$$\frac{S_{\nu,\rm arc}}{f_\nu} \propto y_0^{1.3,\,1.4}\ , \tag{5}$$

[5] Throughout the paper we often compare scaling relations at $z = 0.2$ and 1.0 for the self-similar and $K_0 = 300$ keV cm^2 models. The choice in redshift is motivated by the fact that most interferometric observations are of clusters with $0.2 \lesssim z \lesssim 1.0$, while the choice in entropy floor level is motivated by X-ray observations that require $K_0 \gtrsim 300$ keV cm^2 for massive clusters.

while the $K_0 = 300$ keV cm^2 model approximately predicts

$$\frac{S_{\nu,\rm arc}}{f_\nu} \propto y_0^{1.0,\,1.1}\ . \tag{6}$$

A more precise analytic expression for the $S_{\nu,\rm arc}/f_\nu$-y_0 relation at any $z \lesssim 1$ and any entropy floor in the range $K_0 \approx 100$–700 keV cm^2 is presented in Table 1.

At a fixed redshift, the presence of an entropy floor flattens the relationship between $S_{\nu,\rm arc}/f_\nu$ and y_0 because clusters with small values of y_0 (i.e., low-mass clusters) are more strongly influenced (relatively speaking) by entropy injection than clusters with large values of y_0.

It is worth noting that, for the most part, the $S_{\nu,\rm arc}$-y_0 relations (and, in fact, virtually every relation discussed in the paper) exhibit almost perfect power-law behavior. This may seem rather surprising in light of the fact that most X-ray scaling relations show some kind of a break from power-law trends (see, e.g., BBLP02). We note, however, that the break in the $L_{\rm X}$-$T_{\rm X}$ relation, for example, occurs at the transition between groups and clusters (roughly $T_{\rm X} \lesssim 1$ keV). This is below the range of temperatures (and central Compton parameters) studied in the present paper. We verify that a break does occur for low-mass systems (i.e., for systems with $y_0 \lesssim 10^{-5}$), but, because such low-mass systems have very weak integrated SZ effect signals, there is little hope of observing this feature in the near future.

In the bottom panel of Figure 2 we plot the $S_{\nu,\rm halo}/f_\nu$-y_0 relations. With the quantity $S_{\nu,\rm halo}/f_\nu$ only slightly affected by the presence of an entropy floor (and, therefore, the relative difference in the normalizations of the models is at a maximum), these relations are more sensitive to entropy injection than those plotted in the top panel of Figure 2. For example, for a $z = 0.2$ cluster with a fixed value of $\log y_0 \approx -3.7$, the $K_0 = 430$ keV cm^2 model predicts a flux density that is roughly 3 times larger than that predicted by

TABLE 1

PARAMETERS FOR SCALING RELATIONS: $Y = A(1+z)^\gamma K_2^\alpha X^\beta$

Relation: Y-X	Parameter	Value
$S_{\nu,\rm arc}/f_\nu$-y_0	A	5.807×10^4
	γ	$-0.244 - 4.812\log K_2 + 1.787(\log K_2)^2$
	α	$0.148 + 0.620z - 0.007z^2$
	β	$1.016 - 0.017\log K_2 + 0.150z - 0.186z\log K_2$
$S_{\nu,\rm halo}/f_\nu$-y_0	A	7.893×10^7
	γ	$-7.486 - 140.076\log K_2 - 0.689(\log K_2)^2$
	α	$0.527 + 52.220z - 10.589z^2$
	β	$1.478 - 0.269\log K_2 - 0.058z - 0.026z\log K_2$
y_0-$M(r_{500})$.....	A	3.568×10^{-21}
	γ	$-1.956 - 88.996\log K_2 - 7.675(\log K_2)^2$
	α	$-3.397 + 35.984z - 8.293z^2$
	β	$1.130 + 0.243\log K_2 + 0.041z + 0.032z\log K_2$
y_0-$T_{\rm X}$.....	A	5.668×10^{-6}
	γ	$0.188 + 1.287\log K_2 - 0.558(\log K_2)^2$
	α	$-0.734 - 0.451z + 0.089z^2$
	β	$1.880 + 0.287\log K_2 + 0.070z - 0.003z\log K_2$
y_0-$L_{\rm X}$.....	A	6.659×10^{-41}
	γ	$1.504 + 24.922\log K_2 + 4.478(\log K_2)^2$
	α	$0.887 - 11.117z + 3.057z^2$
	β	$0.805 - 0.022\log K_2 - 0.005z - 0.010z\log K_2$

NOTE.—$K_2 \equiv K_0/100$ keV cm^2. Note that the relations are accurate to better than the $\approx$5% level over the ranges $0.1 \lesssim z \lesssim 1$ and 100 keV cm^2 $\lesssim K_0 \lesssim$ 700 keV cm^2.

the self-similar model (as opposed to being only about 2 times larger for the relation presented in the top panel).

The steepness of the relation is also altered by an entropy floor. Using simple scaling arguments, one can easily arrive at the predicted self-similar result. Combining $S_{\nu,\mathrm{halo}}/f_\nu \propto T_X R^3$ and $y_0 \propto T_X R$ with $R \propto T_X^{0.5}$ (which is just the virial theorem) yields

$$\frac{S_{\nu,\mathrm{halo}}}{f_\nu} \propto y_0^{5/3} , \tag{7}$$

in excellent agreement with the predictions of the BBLP02 isothermal model. However, injection of entropy flattens the relation, and at $z = 0.2$ and 1.0, the $K_0 = 300$ keV cm^2 model approximately predicts

$$\frac{S_{\nu,\mathrm{halo}}}{f_\nu} \propto y_0^{1.3,\,1.2} . \tag{8}$$

An analytic expression for the $S_{\nu,\mathrm{halo}}/f_\nu$-$y_0$ relation at any $z \lesssim 1$ and any entropy floor between 100 keV cm$^2 \lesssim K_0 \lesssim 700$ keV cm^2 is given in Table 1.

Since the $S_{\nu,\mathrm{halo}}/f_\nu$-$y_0$ relation is more sensitive to entropy injection (relatively speaking) than the $S_{\nu,\mathrm{arc}}/f_\nu$-$y_0$ relation, this means that observations obtained with future experiments, such as SZA, AMiBA, and AMI (which will probe larger angular scales than that of current interferometers), will (at least in theory) have the best chance of placing tight constraints on the nongravitational entropy of high-redshift clusters.

We note that most of the dependence of the relations plotted in Figure 2 (both the top and bottom panels) on the entropy floor level, K_0, is due to the central Compton parameter, y_0. A completely resolved central decrement formally requires infinite resolution, and there is little to be gained by increasing the resolution beyond the smallest scale on which the cluster structure varies. For diffuse emission, higher resolution normally means less signal per resolution element, so pushing to very high resolution will not lead to much new information. Alternatively, the central Compton parameter can be estimated by fitting a model (e.g., the isothermal β model) to the observed SZ effect surface brightness and extrapolating it to the cluster center (as discussed briefly in § 3). This method is widely used to estimate y_0 (e.g., Carlstrom, Joy, & Grego 1996; Holzapfel et al. 1997; Grego et al. 2000, 2001; Reese et al. 2000, 2002; Pointecouteau et al. 2001, 2002; Jones et al. 2002; Grainge et al. 2002). While the *statistical* measurement error on y_0 for current data is typically only of order 100 μK (which is relatively small compared to the differences between the models plotted in Fig. 2, assuming that S_ν/f_ν is known), it has yet to be demonstrated that the *systematic* error (due to assuming an incorrect surface brightness model) for current data is negligible. If the models employed in the extrapolation provide poor descriptions of the surface brightness profiles, then one would expect the results to vary as a function of instrument characteristics (e.g., resolution, field of view). However, a comparison of the results of various studies (which made use of different instruments; e.g., Ryle telescope, BIMA/OVRO, and SuZIE) of the same clusters reveals that the agreement is quite good, often within 1 σ statistical uncertainty (see, e.g., Holzapfel et al. 1997; Reese et al. 2002; Jones et al. 2002). Thus, the extrapolation procedure seems to be a viable way of estimating the central Compton parameter at current sensitivity. By modeling "mock" (future) SZA observations, we also demonstrated that this extrapolation procedure is an accurate way of estimating the true underlying values of y_0 and S_ν of the BBLP02 cluster models (see McCarthy et al. 2003).

Finally, we point out that part of the motivation for our study of the S_ν-y_0 relations (and the other scaling relations involving these quantities) comes from the fact that observational studies often use either S_ν or y_0 to characterize a cluster's SZ effect but not usually both. For example, integrated SZ effect flux densities are often associated with large-beam single-dish experiments, while estimates of the central Compton parameter normally come from high-resolution interferometric observations. However, if one is able to determine $y(\theta)$ (i.e., the SZ effect "surface brightness" profile) from a single data set, then, strictly speaking, it is not necessary to use scaling relations to probe the entropy of the ICM. For example, the SZ effect surface brightness profile could be used together with the X-ray surface brightness profile (if it is known) to determine the true three-dimensional entropy distribution of the gas (with some assumptions about the geometry of the cluster). The disadvantages of this method are as follows: (1) it requires X-ray observations, and (2) it probably cannot be used for the most distant clusters, since the X-ray signal-to-noise ratio falls sharply with increasing z. Alternatively, the entropy distribution could be constrained by comparing the observed SZ effect surface brightness profile with theoretically predicted profiles. This is similar to using scaling relations, since the entropy distribution is being inferred and not measured, but with the important difference that all of the available SZ effect information, $y(\theta)$, is being used in the comparison. We are in the process of exploring these methods, and they will be addressed in detail in a subsequent paper. For now, we stick with the scaling relations derived above, which are more readily comparable with available observations.

4.2. *The y_0–X-Ray Scaling Relations*

4.2.1. y_0-$M(r_{500})$

In Figure 3 we present scaling relations between y_0 and the total cluster dark matter mass within the radius r_{500} [i.e., $M(r_{500})$]. This is the radius within which the mean dark matter mass density is 500 times the critical density at $z = 0$. The lines hold the same meaning as in Figure 2. For clarity, we plot the $z = 0.2$ predictions in the left-hand panel and the $z = 1.0$ predictions in the right-hand panel.

It is apparent that entropy injection has a substantial effect on the y_0-$M(r_{500})$ relation. Both the normalization and the steepness of the relation are modified. First, the normalizations imply that, for a cluster of given mass at a given redshift, entropy injection tends to diminish the strength of y_0. For example, at $z = 0.2$, a cluster with $M(r_{500}) \approx 9 \times 10^{14}$ $M_\odot$ will have $y_0 \approx 4 \times 10^{-4}$ in the absence of an entropy floor, but the central Compton parameter is only half this value for an entropy floor of $K_0 \approx 430$ keV cm^2. This corresponds to a difference of nearly 1060 μK at 30 GHz (which is large compared to the typical BIMA/OVRO statistical measurement error of 100–200 μK; Reese et al. 2000, 2002). Of course, there will also be a measurement error associated with the cluster mass. Typically, X-ray–determined masses have associated statistical uncertainties of about 20% (Nevalainen et al. 2000; Finoguenov et al. 2001). Therefore,

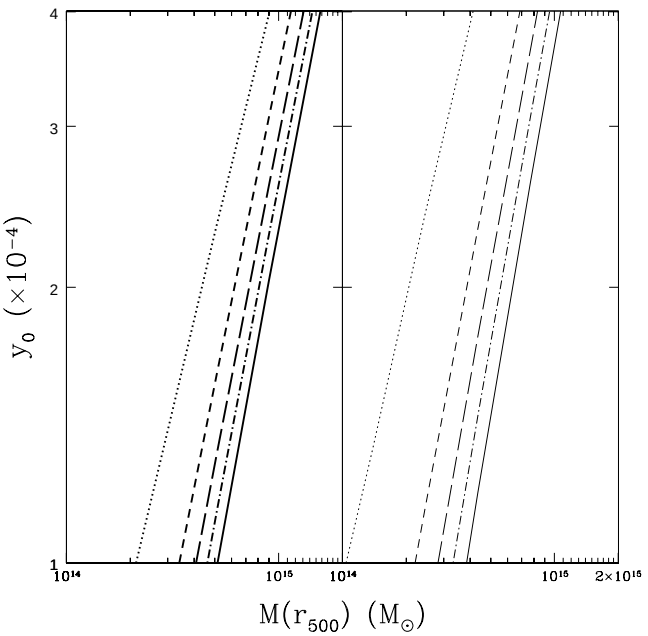


FIG. 3.—Comparison of the y_0-$M(r_{500})$ relations. The lines hold the same meanings as in Fig. 2. *Left:* $z = 0.2$. *Right:* $z = 1.0$.

based on Figure 3, it should be possible to constrain K_0 to within about ± 100 keV cm^2 with current data.

Physically, the diminution in the normalization y_0-$M(r_{500})$ relation can be understood since entropy injection greatly reduces the pressure of the cluster gas near the core (and therefore y_0; see Fig. 1) but does not affect its dark matter mass. It is also worth noting that the normalizations of the individual models are a function of redshift. For example, the $K_0 = 100$ keV cm^2 at $z = 0.2$ predicts a relation somewhat similar to that of the $K_0 = 200$ keV cm^2 at $z = 0.5$ or the $K_0 = 430$ keV cm^2 at $z = 1.0$. Thus, it is extremely important to consider the evolution of galaxy clusters when comparisons are made to observational data (i.e., information about the redshift of the clusters is required in order to constrain the level of the entropy floor).

Another interesting point is that the difference between the normalizations of the models becomes greater at higher redshift. For example, the difference between y_0 for the isothermal and $K_0 = 100$ keV cm^2 models of an $M(r_{500}) \approx 5.6 \times 10^{14}\ M_\odot$ cluster at $z = 1.0$ is about 3.7 times larger than at $z = 0.2$. This is a result of the fact that the physical size of the isentropic core (r_c; discussed in § 2) is a larger fraction of the cluster virial radius at higher redshifts. This trend of increasing $r_c/R_{\rm halo}$ with redshift can be understood as follows. In BBLP02, it was pointed out that there is a critical mass threshold that determines the importance of gravitational shock heating. For clusters with masses above this threshold, shock heating significantly increases the entropy of the intracluster gas and it begins to dominate the injected nongravitational entropy (except for in the very central regions of the clusters). For clusters with masses below this threshold, shock heating is unimportant. The critical mass also sets the size of the isentropic core, r_c. Incorporating the results of recent high-resolution hydrodynamic simulations (Lewis et al. 2000), BBLP02 defined the critical mass to be that which gives rise to a gas temperature at $R_{\rm halo}$ that is equal to one-half of the cluster virial temperature. Using this constraint, it is relatively straightforward to show that the critical mass (for a fixed entropy floor level) increases with redshift and, therefore, so does the ratio $r_c/R_{\rm halo}$. For gas in the core of the cluster (with entropy equal to K_0), $P_{\rm core} \propto \rho_{\rm core}^{5/3}$ and, therefore, $T_{\rm core} \propto \rho_{\rm core}^{2/3}$. At high redshifts, the cluster gas is denser and, in the case of an $\Omega_m = 1$ universe (assumed here for simplicity), scales as $\rho \propto (1+z)^3$. Therefore, the temperature of the gas in the core scales as $T_{\rm core} \propto (1+z)^2$. The gas temperature at the virial radius, on the other hand, scales as $T_{\rm halo} \propto (1+z)$. Thus, the ratio $T_{\rm core}/T_{\rm halo}$ increases with redshift, and in order to match the temperature constraint described above, the critical mass threshold and $r_c/R_{\rm halo}$ must increase with z as well.

The steepness of the y_0-$M(r_{500})$ relation is also affected by an entropy floor. If clusters are self-similar, then $y_0 \propto T_{\rm X}R$, $R \propto T_{\rm X}^{0.5}$, and $M(r_{500}) \propto T_{\rm X}^{1.50}$ (Evrard et al. 1996). This leads to

$$y_0 \propto M(r_{500})\ , \tag{9}$$

while at $z = 0.2$ and 1.0, the $K_0 = 300$ keV cm^2 model predicts

$$y_0 \propto M(r_{500})^{1.3,\,1.3}\ . \tag{10}$$

A more precise form of the y_0-$M(r_{500})$ relation as a function of both the entropy floor (K_0) and redshift is presented in Table 1 [valid for $M(r_{500}) \gtrsim 1.5 \times 10^{14}\ M_\odot$].

The steepening of the relation with the increase in the level of the entropy floor can also be understood in an intuitive sense. It stems from the fact that the relative decrease in the gas pressure at the cluster center is strongest for low-mass clusters (which have the shallowest potential wells; see Fig. 1).

Again, because of the increasing importance of entropy injection as one goes to low masses, a break from power-law behavior in the y_0-$M(r_{500})$ relation occurs at the transition between groups and clusters (not shown). For entropy floors of $K_0 \gtrsim 300$ keV cm^2, the break becomes quite noticeable for systems with $M(r_{500}) \lesssim 8 \times 10^{13}\ M_\odot$, which is below the range of system masses that we are most interested in and far below the range of system masses that can be observed presently.

We have found that, at least theoretically, the best hope for testing galaxy clusters for the presence of excess entropy using the y_0-$M(r_{500})$ relation is at high redshift, although our results reveal that the relation is sensitive to the entropy floor level even at low redshifts. The quantity $M(r_{500})$ is usually determined through X-ray observations (e.g., Ettori & Fabian 1999); hence, we have placed it in the "y_0–X-ray scaling relations" subsection. However, gravitational lensing has also been used recently to trace the mass profiles of clusters out to radii near or exceeding that of r_{500} with statistical uncertainties similar to that of X-ray–determined masses (e.g., Clowe & Schneider 2001; Gray et al. 2002; Athreya et al. 2002). Thus, like the S_ν-y_0 relation, the y_0-$M(r_{500})$ relation can also potentially be measured completely independent of X-ray results.

4.2.2. y_0-$T_{\rm X}$

In Figure 4 we present scaling relations between y_0 and the mean emission-weighted gas temperature ($T_{\rm X}$) of a cluster. The lines hold the same meaning as in Figure 2. Of the scaling relations presented thus far, the y_0-$T_{\rm X}$

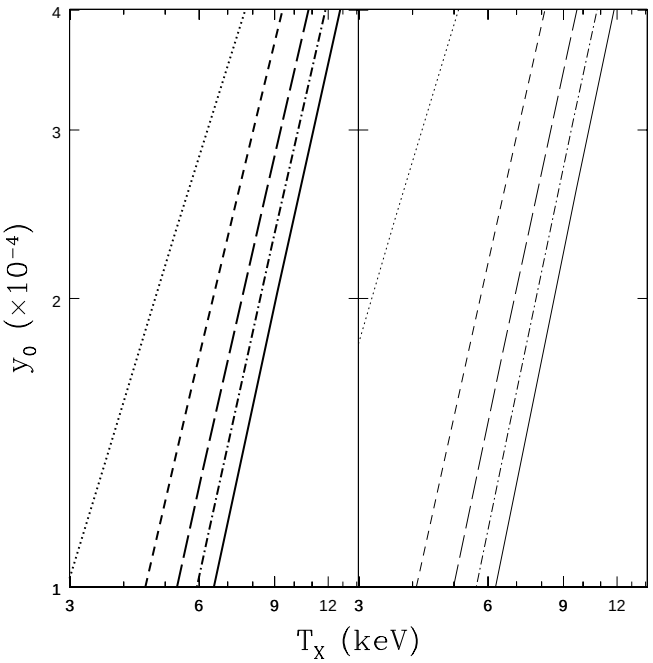


FIG. 4.—Comparison of the y_0-T_X relations. The lines hold the same meanings as in Fig. 2. *Left:* $z = 0.2$. *Right:* $z = 1.0$.

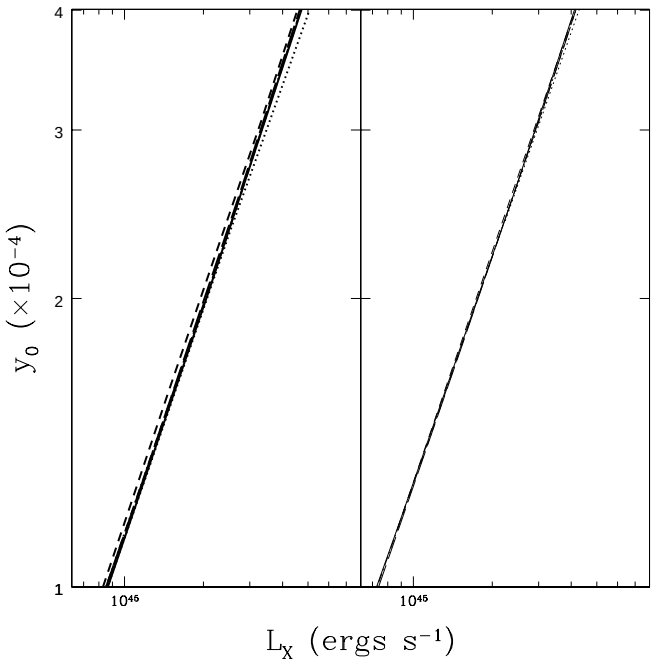


FIG. 5.—Comparison of the y_0-L_X relations. The lines hold the same meanings as in Fig. 2. *Left:* $z = 0.2$. *Right:* $z = 1.0$.

relation is the most sensitive to the entropy floor level. There is a twofold effect in that entropy injection diminishes y_0 but also *increases* T_X for a cluster of mass M (see, e.g., Fig. 1 of MBB02). For example, at $z = 0.2$, a cluster that has $T_X \approx 7$ keV and no entropy floor will have a value of y_0 that is about 3.5 times larger than a cluster (also with $T_X \approx 7$ keV) that has an entropy floor of $K_0 \approx 430$ keV cm^2. At 30 GHz, this corresponds to a difference of $\approx$1300 μK. Current SZ effect and X-ray data can constrain the central decrement (Compton parameter) and emission-weighted temperature of massive clusters at about the 10% level (e.g., Reese et al. 2002), making the y_0-T_X relation an extremely promising test of nongravitational entropy injection. Furthermore, the difference in the normalizations becomes progressively larger with increasing redshift.

The slopes of the predicted relations are also very sensitive to the level of entropy injection. Combining $y_0 \propto T_X R$ with $R \propto T_X^{0.5}$ yields the self-similar result

$$y_0 \propto T_X^{3/2} , \tag{11}$$

while at $z = 0.2$ and 1.0, the $K_0 = 300$ keV cm^2 model predicts

$$y_0 \propto T_X^{2.0,\,2.1} . \tag{12}$$

An analytic expression for the y_0-L_X relation as a function of both the entropy floor (K_0) and redshift is presented in Table 1 (valid for $T_X \gtrsim 3$ keV).

Lastly, we note that a break in slope of the relations occurs at $T_X \lesssim 1$ keV, in good qualitative agreement with the position and steepness of the break found in the y-T relation of Cavaliere & Menci (2001; see their Fig. 4). Unfortunately, present SZ effect observations are essentially limited to systems with $T_X \gtrsim 5$ keV.

4.2.3. y_0-L_X

In Figure 5 we plot scaling relations between the central y parameter and the total bolometric X-ray luminosity (L_X) of a cluster. The lines hold the same meaning as in Figure 2. These relations are more complicated than those presented immediately above because both of the coordinates, y_0 and L_X, are affected by entropy injection. Very interestingly, however, the y_0-L_X relation is almost unchanged by the addition of an entropy floor. Both the self-similar and entropy floor models predict very similar slopes and normalizations (at all redshifts). At first sight, this may seem rather surprising. However, the predicted y_0-L_X relations can be understood as follows. The luminosity of a cluster of fixed mass is reduced by entropy injection because $L_X \propto n_e^2$ and entropy injection greatly reduces the gas density near the cluster core, where most of the X-ray emission originates. In the case of the BBLP02 entropy floor models, the result is that $L_X \propto M^{1.5}$, roughly (instead of $L_X \propto M^{4/3}$ in the self-similar case). On the other hand, we showed in § 4.2.1 that an increase in the entropy floor level strongly diminishes y_0 for a cluster of fixed mass, and this leads to $y_0 \propto M^{1.3}$. This implies that entropy injection gives rise to $y_0 \propto L_X^{0.8}$ (roughly), which is very close to the self-similar scaling of

$$y_0 \propto L_X^{3/4} . \tag{13}$$

A precise analytic expression for the y_0-L_X relation as a function of both the entropy floor (K_0) and redshift is presented in Table 1 (valid for $L_X \gtrsim 10^{44}$ ergs s^{-1}).

Despite being insensitive to the entropy floor level, the y_0-L_X relation has at least two other potential uses. First, it could be used as a consistency check of other X-ray and SZ effect scaling relations. Second, it could allow one to deduce the X-ray luminosity of clusters in cases in which only SZ effect observations are available (or vice versa) without

having to worry about the role of "additional" gas physics. The accuracy of this will be limited by the relatively large amount of intrinsic scatter present in the X-ray luminosities of clusters (see, e.g., studies of the L_X-T_X relation; Markevitch 1998; Novicki, Sornig, & Henry 2002) and by the measurement errors associated with y_0.

4.3. S_ν–X-Ray Scaling Relations

Apart from the central y parameter, we also investigated theoretical scaling relations between the frequency-independent integrated SZ effect flux density and the X-ray observables $M(r_{500})$, L_X, and T_X. Again, we evaluated S_ν/f_ν within a fixed angular radius of $1'$ and within R_{halo}. Since these relations can be reconstructed from Figures 2–5 or Table 1, we summarize the important points here only.

For the very same reasons discussed in § 4.2.1, the S_ν/f_ν-$M(r_{500})$ relation has its normalization decreased by entropy injection and, also, the relation becomes steeper. How large these effects will be depends on which radius S_ν/f_ν is evaluated within. Because the dark matter mass is unaffected by entropy injection, the S_ν/f_ν-$M(r_{500})$ relation will *always* be most strongly modified if S_ν/f_ν is evaluated within small projected radii (where entropy injection is most prevalent). Thus, evaluating S_ν/f_ν within the central $1'$ provides a more sensitive test of the entropy floor than if S_ν/f_ν is measured within R_{halo}. Of course, it follows that the y_0-$M(r_{500})$ relation is the most sensitive to the entropy floor level of any and all of the SZ effect–$M(r_{500})$ relations. The S_ν/f_ν-$M(r_{500})$ relation, however, could offer a useful consistency check.

The S_ν/f_ν-T_X relation also becomes steeper and has its normalization decreased with increasing values of K_0 (S_ν/f_ν is diminished while T_X is increased). The maximum (relative) difference between the various models occurs when the SZ effect flux densities are measured within small projected radii, although the increase in T_X is large enough such that the relation is sensitive to the entropy floor level even when S_ν/f_ν is measured within R_{halo}. Again, these relations offer useful consistency checks of the more entropy floor–sensitive y_0-T_X relation.

Finally, entropy injection has an interesting effect on the S_ν/f_ν-L_X relation.[6] Both the SZ effect flux density and the luminosity are reduced as the level of entropy injected is increased, similar to the y_0-L_X relation. However, in the case of the present relation, the reduction in the luminosity is greater than the reduction in the SZ effect flux density (relatively speaking). This is because S_ν is much less sensitive than y_0 to the entropy floor level, K_0. The result is that the normalization of the S_ν/f_ν-L_X relation is increased by entropy injection. The sensitivity of this relation to the entropy floor level depends on what radius the flux density is evaluated within. It is most sensitive when S_ν is integrated out to R_{halo}, since the relative reduction in S_ν is at a minimum. It is least sensitive when the SZ effect is evaluated at zero projected radius (i.e., y_0-L_X).

5. DISCUSSION AND CONCLUSIONS

Comparisons of observed and predicted cluster X-ray scaling relations have led to suggestions that important (nongravitational) gas physics is being neglected in analytic models and numerical simulations. It has been found that the presence of a core in the entropy profiles of clusters (which may be generated through heating and/or cooling processes) can account for the deviations between observations and theory (e.g., Bower 1997; Balogh et al. 1999; Ponman et al. 1999; Wu et al. 2000; Lloyd-Davies et al. 2000, 2002; Tozzi & Norman 2001; Bialek, Evrard, & Mohr 2001; Borgani et al. 2001; Voit & Bryan 2001; BBLP02; MBB02; Voit et al. 2002; Davé et al. 2002). So far, X-ray observations have provided the only evidence for this excess entropy, and it has come from low-redshift ($z \lesssim 0.2$) clusters alone. Cosmological dimming is partially responsible for the lack of information on the entropy of more distant groups/clusters.

In the interest of achieving a better physical understanding of important nongravitational processes in high-redshift clusters (and how these processes affect cluster formation and evolution), we have derived a number of theoretical scaling relations based on SZ effect quantities and have analyzed how these relations are modified by the addition of an entropy floor. We find that entropy injection reduces the gas pressure in the cores of clusters and, therefore, diminishes the amplitude of both the central and integrated Compton parameters (which are directly proportional to the SZ effect). This translates to a steepening of and a reduction in the normalization of the y_0-$M(r_{500})$ and S_ν/f_ν-$M(r_{500})$ relations. Scaling relations between the Compton parameter(s) and X-ray temperature or luminosity are more complicated because both T_X and L_X are also affected by entropy injection (whereas the cluster mass M is not). Because T_X is increased by an entropy floor, the y_0-T_X and S_ν/f_ν-T_X relations have their normalizations severely reduced by entropy injection. These relations are also considerably steeper than in the case in which no entropy floor is present (i.e., the isothermal self-similar model). On the other hand, because L_X is decreased with entropy injection, the y_0-L_X relation is almost unaffected by entropy injection, while the normalization of the S_ν/f_ν-L_X relation is increased by entropy injection. Finally, the S_ν/f_ν-y_0, a relation that can (in principle) be measured entirely through SZ effect observations, has its normalization increased by an entropy floor (the relative reduction in y_0 is much greater than in S_ν/f_ν). The relation is also slightly flattened. Analytic expressions for these relations as a function of entropy floor level and redshift can be found in Table 1.

We are aware of only two other studies that have examined the effects of an entropy floor on cluster SZ effect scaling relations: Holder & Carlstrom (2001) and Cavaliere & Menci (2001). Using simplified cluster models, Holder & Carlstrom (2001) illustrated the potential power of high-z SZ effect observations when it comes to studying the physics of ICM. Their Figure 1 shows the impact of an entropy floor on the central SZ effect decrement–cluster core radius relation at $0.5 \leq z \leq 2.0$. They find that the addition of an entropy floor tends to decrease the central decrement and increase the cluster core radius for clusters of a fixed total mass. This is in very good qualitative agreement with our Figure 3, which illustrates that the normalization of the y_0-$M(r_{500})$ relation is decreased by entropy injection, and also with our Figure 2, which demonstrates that for clusters of a fixed y_0, the SZ effect flux density is increased by an entropy floor and, therefore, the SZ effect surface brightness becomes less centrally peaked (i.e., the core radius grows).

[6] Note that there is an error in Fig. 12 of the original BBLP02 publication. The self-similar predictions were incorrectly plotted.

Cavaliere & Menci (2001), on the other hand, implemented a semianalytic model of galaxy formation and clustering and computed a *present-day* y-T_X scaling relation and analyzed how it was modified by entropy injection from stellar winds and supernova blasts. In qualitative agreement with the results presented in § 4, these authors found that entropy injection tends to diminish the Compton parameter for a cluster of given mean emission-weighted temperature, T_X. However, our theoretical results are not directly comparable to those of Cavaliere & Menci (2001) since their focus was mainly on nearby ($z = 0$) groups, whereas we have investigated massive, distant clusters such as those regularly observed by the BIMA/OVRO arrays and the Ryle telescope. We also point out that the majority of clusters expected to be found in upcoming "blind" surveys will be at high redshift ($z \sim 1$; Holder et al. 2000). Finally, the Cavaliere & Menci (2001) cluster models only invoked low levels of entropy injection ($K_0 < 100$ keV cm^2) consistent with measurements of nearby groups (Ponman et al. 1999; Lloyd-Davies et al. 2000), whereas we have generally focused on higher levels of entropy injection (which are required to match X-ray observations of nearby massive clusters; Tozzi & Norman 2001; BBLP02; MBB02).

One thing we have not addressed in the present study is the effect of radiative cooling on SZ effect scaling relations. Correctly modeling the effects of radiative cooling in numerical simulations and analytic cluster models is a daunting task (see Balogh et al. 2001 for a detailed study of the "cooling crisis"). Cooling can significantly modify not only the ICM density and temperature distributions but also the underlying dark matter distribution of clusters (see, e.g., Fig. 12 of Lewis et al. 2000). In addition, cooling gives rise to other "subgrid" processes such as star formation, outflows, and supernova explosions. These will also modify the ICM's structure and appearance. While modeling this is quite difficult, we know from both optical and X-ray observations of clusters that cooling must be occurring, at least at some level, and, ultimately, must be modeled correctly in order to attain a deep physical understanding of the observed properties of clusters. Numerical simulations and analytic models that attempt to take this complicated process into account (e.g., Voit & Bryan 2001; da Silva et al. 2001; Wu & Xue 2002; Voit et al. 2002; Davé et al. 2002; White et al. 2002) are apparently able to match many of the features of the X-ray scaling relations of nearby clusters. In this sense, cooling has very similar effects on the ICM to those induced by "preheating." Cooling has an advantage over preheating in that it does not require some (as of yet) unknown source to transfer large amounts of energy into the ICM. However, cooling alone leads to an expected amount of cooled gas in groups and clusters that far exceeds what is observed (Balogh et al. 2001). Feedback, be it through preheating or heating after cluster formation, must also be an important process.

We are currently in the process of adding radiative cooling to the BBLP02 analytic models (I. G. McCarthy et al. 2003, in preparation) with the intention of exploring how SZ effect and X-ray scaling relations are modified by it. As far as we know, the effects of cooling on SZ effect scaling relations have not yet been examined. While, in general, we do not expect the results of the present study to change significantly with the inclusion of cooling (since cooling affects the ICM in a very similar way to that of preheating), in detail we do anticipate subtle (or perhaps not so subtle) differences to be present. This may also lead to a way of separating out the relative contributions of cooling and heating to cluster scalings.

Finally, we note that with the recent release of the Reese et al. (2002) data, there are now enough SZ effect observations to begin testing the "entropy floor" hypothesis by mapping out the various correlations involving the SZ and X-ray observables and comparing these to their theoretical counterparts derived in this paper. It would be most interesting to see if these correlations also favor the existence of an entropy floor and whether the level of this floor is comparable to that required to explain the X-ray trends. This will be the focus of McCarthy et al. (2003), a companion paper to this one.

We thank the referee for very useful comments and suggestions. We also thank Peng Oh, Kathy Romer, and Mark Voit for helpful discussions. A. B. would like to acknowledge the hospitality extended to him by the Canadian Institute for Theoretical Astrophysics during his tenure as CITA Senior Fellow. I. G. M. is supported by a postgraduate scholarship from the Natural Sciences and Engineering Research Council of Canada (NSERC). A. B. is supported by an NSERC operating grant, G. P. H. is supported by the W. M. Keck Foundation, and M. L. B. is supported by a PPARC rolling grant for extragalactic astronomy and cosmology at the University of Durham.

REFERENCES

Allen, S. W., & Fabian, A. C. 1998, MNRAS, 297, L57
Arnaud, M., & Evrard, A. E. 1999, MNRAS, 305, 631
Athreya, R. M., et al. 2002, A&A, 384, 743
Babul, A., Balogh, M. L., Lewis, G. F., & Poole, G. B. 2002, MNRAS, 330, 329 (BBLP02)
Balogh, M. L., Babul, A., & Patton, D. R. 1999, MNRAS, 307, 463
Balogh, M. L., Pearce, F. R., Bower, R. G., & Kay, S. T. 2001, MNRAS, 326, 1228
Bialek, J. J., Evrard, A. E., & Mohr, J. J. 2001, ApJ, 555, 597
Birkinshaw, M. 1999, Phys. Rep., 310, 97
Borgani, S., et al. 2001, ApJ, 559, L71
Bower, R. G. 1997, MNRAS, 288, 355
Bryan, G. L. 2000, ApJ, 544, L1
Burles, S., Nollett, K. M., & Turner, M. S. 2001, ApJ, 552, L1
Carlstrom, J. E., Joy, M., & Grego, L. 1996, ApJ, 456, L75
Cavaliere, A., & Fusco-Femiano, R. 1976, A&A, 49, 137
———. 1978, A&A, 70, 677
Cavaliere, A., & Menci, N. 2001, MNRAS, 327, 488
Clowe, D., & Schneider, P. 2001, A&A, 379, 384
da Silva, A. C., et al. 2001, ApJ, 561, L15
Davé, R., Katz, N., & Weinberg, D. H. 2002, ApJ, 579, 23
Ettori, S., & Fabian, A. C. 1999, MNRAS, 305, 834
Evrard, A. E., & Henry, J. P. 1991, ApJ, 383, 95
Evrard, A. E., Metzler, C. A., & Navarro, J. F. 1996, ApJ, 469, 494
Finoguenov, A., Reiprich, T. H., & Böhringer, H. 2001, A&A, 368, 749
Fixsen, D. J., et al. 1996, ApJ, 473, 576
Grainge, K., et al. 2002, MNRAS, 329, 890
Gray, M. E., et al. 2002, ApJ, 568, 141
Grego, L., et al. 2000, ApJ, 539, 39
———. 2001, ApJ, 552, 2
Holder, G. P., & Carlstrom, J. E. 2001, ApJ, 558, 515
Holder, G. P., et al. 2000, ApJ, 544, 629
Holzapfel, W., et al. 1997, ApJ, 480, 449
Horner, D. J., Mushotzky, R. F., & Scharf, C. A. 1999, ApJ, 520, 78
Jones, M. E., et al. 2002, MNRAS, submitted
Kaiser, N. 1991, ApJ, 383, 104
Lewis, G. F., et al. 2000, ApJ, 536, 623
Lloyd-Davies, E. J., Bower, R. G., & Ponman, T. J. 2002, MNRAS, submitted
Lloyd-Davies, E. J., Ponman, T. J., & Cannon, D. B. 2000, MNRAS, 315, 689
Loewenstein, M. 2000, ApJ, 532, 17

Markevitch, M. 1998, ApJ, 504, 27
McCarthy, I. G., Babul, A., & Balogh, M. L. 2002, ApJ, 573, 515 (MBB02)
McCarthy, I. G., Holder, G. P., Babul, A., & Balogh, M. L. 2003, ApJ, 591, 526
Mohr, J. J., Mathiesen, B., & Evrard, A. E. 1999, ApJ, 517, 627
Moore, B., et al. 1998, ApJ, 499, L5
Nath, B. B., & Roychowdhury, S. 2002, MNRAS, 333, 145
Nevalainen, J., Markevitch, M., & Forman, W. 2000, ApJ, 532, 694
Novicki, M. C., Sornig, M., & Henry, J. P. 2002, AJ, 124, 2413
Pointecouteau, E., et al. 2001, ApJ, 552, 42
———. 2002, A&A, 387, 56
Ponman, T. J., Cannon, D. B., & Navarro, J. F. 1999, Nature, 397, 135
Reese, E. D., et al. 2000, ApJ, 533, 38
———. 2002, ApJ, 581, 53
Springel, V., White, M., & Hernquist, L. 2001, ApJ, 549, 681
Sunyaev, R., & Zeldovich, Y. 1970, Comments Astrophys. Space Phys., 2, 66
———. 1980, MNRAS, 190, 413
Thomas, P. A., Muanwong, O., Kay, S. T., & Liddle, A. R. 2002, MNRAS, 330, L48
Tozzi, P., & Norman, C. 2001, ApJ, 546, 63
Vikhlinin, A., Forman, W., & Jones, C. 1999, ApJ, 525, 47
Voit, M. G., & Bryan, G. L. 2001, Nature, 414, 425
Voit, M. G., Bryan, G. L., Balogh, M. L., & Bower, R. G. 2002, ApJ, 576, 601
White, M., Hernquist, L., & Springel, V. 2002, ApJ, 579, 16
Wu, K. K. S., Fabian, A. C., & Nulsen, P. E. J. 2000, MNRAS, 318, 889
Wu, X., & Xue, Y. 2002, ApJ, 572, L19